PROCEEDINGS OF SCIENCE

Universal behavior of cumulants in non-equilibrium phase transitions - Kibble-Zurek scaling functions for trans-critical quenches

Mattis Harhoff,[a,*] **Leon J. Sieke,**[b] **Sören Schlichting**[a] **and Lorenz von Smekal**[b,c]

[a] *Fakultät für Physik, Universität Bielefeld, 33615 Bielefeld, Germany*

[b] *Institut für Theoretische Physik, Justus-Liebig-Universität, Heinrich-Buff-Ring 16, 35392 Gießen, Germany*

[c] *Helmholtz Forschungsakademie Hessen für FAIR (HFHF), Campus Gießen, 35392 Gießen, Germany*

E-mail: mharhoff@physik.uni-bielefeld.de, leon.j.sieke@physik.uni-giessen.de, sschlichting@physik.uni-bielefeld.de, lorenz.smekal@physik.uni-giessen.de

In context of the search for the QCD critical endpoint in heavy-ion collisions, a deep understanding of the out-of-equilibrium dynamics of the system is necessary to make well-grounded predictions for signatures in final states. To this end, we investigate the dynamic critical behavior of a classical scalar field theory with $\mathbb{Z}_2$ symmetry in the dynamic universality class of Model A in two spatial dimensions. The critical dynamics of the system is studied under a linear quench protocol, in which the external symmetry breaking field is changed at a constant rate through the critical point. We discuss the connection to the Kibble-Zurek mechanism and determine universal scaling functions, which fully describe the non-equilibrium evolution of the system near the critical point for all quench rates under consideration. We find that, while the scaling functions are non-trivial, the corresponding scaling exponents are fully determined by static critical exponents and the dynamic critical exponent.

FAIR next generation scientists - 8th Edition Workshop (FAIRness2024)
23-27 September 2024
Donji Seget, Croatia

*Speaker

 ISSN 1824-8039 . Published by SISSA Medialab.

PoS(FAIRness2024)014

1. Introduction

In recent years, large theoretical and experimental efforts are being undertaken in order to verify the conjectured existence of a critical endpoint at the end of a first-order transition line in the phase diagram of Quantum Chromo-Dynamics (QCD). This raises the question how signatures of such structures could arise in the context of heavy-ion collisions, in which the system evolves rapidly and out-of-equilibrium [1]. In order to address this question, a deep understanding of non-equilibrium phase transitions is necessary.

Due to a diverging correlation length ξ, systems at critical points become independent of details of their microscopic interactions, such that some of their properties (critical exponents, scaling functions, amplitude ratios etc.) fall into universality classes based on symmetries and dimensionality of the system [2]. Due to a divergence of the relaxation time $\xi_t \sim \xi^z$ (with z being the dynamic critical exponent), the same holds true for dynamics, with the static universality classes splitting up into dynamic universality classes depending on e.g. conservation laws in the system [2, 3]. Due to the diverging relaxation time, the dynamics near a critical point can become arbitrarily slow, referred to as critical slowing down, and the system is actually guaranteed to fall out-of-equilibrium if it comes close enough to the critical point. Universal dynamic quantities include the dynamic critical exponent z, as well as scaling functions fully describing the associated non-equilibrium processes [2, 3]. Universality is thus a powerful tool in the analysis of non-equilibrium dynamics, especially since universal properties of a QCD critical region could be calculated in simpler models of the same universality class, which is believed to be $\mathbb{Z}_2$ with Model H dynamics [4].

In this work, we consider a field theory in the same $\mathbb{Z}_2$ Ising static universality class with much simpler Model A Langevin dynamics in the classification by Halperin and Hohenberg [3], and extract universal quantities such as non-equilibrium scaling functions. In particular, we consider a protocol of trans-critical linear magnetic quenches and describe the dynamics in context of the well-established Kibble-Zurek mechanism [5–7]. The contents of this proceeding are based on the results of [8], to which we refer for a more detailed discussion.

2. Model

We consider a relativistic field theory with quartic interactions in d spatial dimensions, consisting of a scalar field ϕ with conjugate momentum field π. The theory is discretized on a cubic lattice with spacing a; the lattice Hamiltonian reads

$$H = \sum_x a^d \left\{ \frac{1}{2}\pi_x^2 + \frac{1}{2a^2}\sum_{y\sim x}\phi_x\phi_y + \left(\frac{m^2}{2}+\frac{d}{a^2}\right)\phi_x^2 + \frac{\lambda}{4!}\phi_x^4 + J(t)\phi_x \right\}, \tag{1}$$

in which the sum $\sum_{y\sim x}$ runs over sites y adjacent to x. We set $m^2 = -1$ and $\lambda = 1$ in the following. The Hamiltonian exhibits a $\mathbb{Z}_2$-symmetry broken by a time-dependent homogeneous external field $J(t)$. The system is coupled to a heatbath of temperature T by employing Model A Langevin-type dynamics as

$$\partial_t\phi_x = \frac{\partial H}{\partial \pi_x}, \quad \partial_t\pi_x = -\frac{\partial H}{\partial \phi_x} - \gamma\pi_x + \sqrt{2\gamma T}\eta_x(t), \tag{2}$$

with η being a Gaussian white noise with zero mean and $\langle \eta_x(t)\eta_y(t')\rangle = a^{-d}\delta_{xy}\delta(t-t')$. We set $\gamma = 1$ and fix the lattice spacing as $a = 1$; all quantities in the following are expressed in appropriate lattice units. Details of the numerical scheme can be found in [8, 9].
Observables include the average order parameter or "magnetization" $\langle M\rangle$ and susceptibility χ

$$\langle M\rangle = \left\langle \frac{1}{V}\sum_x \phi_x \right\rangle, \qquad \chi = \frac{V}{T}\left(\langle M^2\rangle - \langle M\rangle^2\right), \tag{3}$$

in which the brackets $\langle\cdot\rangle$ denote ensemble averages, as well as higher-order cumulants of the order parameter such as the skewness κ_3 and kurtosis κ_4:

$$\kappa_3 = \left(\frac{V}{T}\right)^2 \left(\langle M^3\rangle - 3\langle M^2\rangle\langle M\rangle + 2\langle M\rangle^3\right) \tag{4}$$

$$\kappa_4 = \left(\frac{V}{T}\right)^3 \left(\langle M^4\rangle - 4\langle M^3\rangle\langle M\rangle - 3\langle M^2\rangle^2 + 12\langle M^2\rangle\langle M\rangle^2 - 6\langle M\rangle^4\right). \tag{5}$$

3. Phase diagram and non-equilibrium dynamics

The model exhibits a ferromagnetic phase diagram as shown in Fig. 1, with a first-order transition line at $J = 0$ and $T < T_c$ discontinuously separating two ordered phases with different sign of $\langle M\rangle$, and a critical point at $J = 0$, $T = T_c$. Static properties of this model and the Ising universality class are well-established in the literature [2, 9–11].

We consider non-equilibrium trajectories in this phase diagram, in which we change the temperature of the heatbath $T(t)$ and the external field $J(t)$ as functions of simulation time t. More specifically, we consider the linear trans-critical magnetic quench protocol

$$T(t) = T_c, \qquad J(t) = -r_J t, \tag{6}$$

in which the system is smoothly forced across the critical point at finite rate r_J. The time scale is set such that $J(t=0) = 0$, such that t can be interpreted as time until the transition.

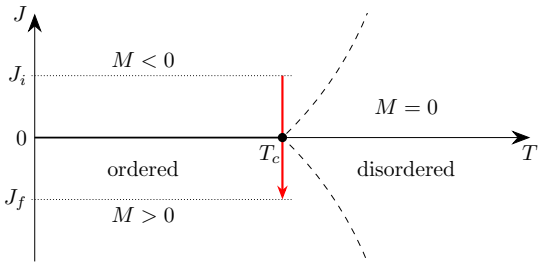

Figure 1: Schematic phase diagram with quench trajectory (6).

We expect the observables along this trajectory to follow their equilibrium values, until, due to critical slowing down, the system inevitably falls out-of-equilibrium near the critical point. After passing the critical point, the system will at some time be able return to equilibrium again.
For this reason, numerically, we let the system thermalize by running the evolution at fixed $T = T_c$, $J > 0$ until the observables stay constant in time, and then start the quench protocol. The initial value of J is chosen such that the system is still in equilibrium at the start of the trajectory at the given r_J.

4. Kibble-Zurek mechanism

The Kibble-Zurek mechanism [5–7] can be used to quantify when and how the system will fall out-of-equilibrium. This will happen roughly when the real rate of change inside the system,

estimated by the normalized rate of change in relaxation time $\dot{\xi}_t/\xi_t$, gets larger than the relaxation rate $1/\xi_t$:

$$\dot{\xi}_t/\xi_t \gtrapprox 1/\xi_t \quad \rightsquigarrow \quad \dot{\xi}_t(t = t_{\mathrm{KZ}}) \equiv 1 \tag{7}$$

The second equality serves as definition of the Kibble-Zurek time t_{KZ}, a proxy for the time when the system falls out-of-equilibrium. Since, until t_{KZ}, the system is in equilibrium, the equilibrium dependence on the critical isotherm $\xi_t \sim J^{-\nu_c z}$ can be used with the exponent ν_c being related to static universal exponents as $\nu_c \equiv \nu/\beta\delta$. Using Eqs. (6) and (7), one can then determine how t_{KZ} and $J_{\mathrm{KZ}} \equiv J(t_{\mathrm{KZ}})$ scale as function of the quench rate r_J in the given protocol:

$$t_{\mathrm{KZ}} \sim r_J^{-\nu_c z/(1+\nu_c z)}, \qquad J_{\mathrm{KZ}} \sim r_J^{1/(1+\nu_c z)} \tag{8}$$

Since, due to the scale invariance at criticality, the values of observables should only depend on t or $J(t)$ and the scale set by r_J, one can make a scaling Ansatz for the value of an arbitrary observable. In a scale transformation $l \to l/s$ with scale parameter $s > 0$, we get for an observable A:

$$A(J, r_J) = A_0 s^{\Delta_A} f_A(s^{1/\nu_c}\bar{J}, s^{z+1/\nu_c}\bar{r_J}) \tag{9}$$

The scaling dimension of A denoted as Δ_A can be extracted from equilibrium scaling laws. f_A denotes a universal scaling function, with $\bar{J} \propto J$ and $\bar{r_J} \propto r_J$ chosen such that the normalization $f(0,1) = f(1,0) = 1$ holds. Choosing the scale s appropriately, one can set the second argument constant, with J/J_{KZ} remaining as first argument. Using the same notation for the scaling function with only one argument, we get e.g.

$$\langle M(J, r_J)\rangle = -M_0 \bar{r_J}^{\beta/(\beta\delta+\nu z)} f_M(J/J_{\mathrm{KZ}}), \tag{10}$$

and analogously for the other observables as described in [8]. It should be emphasized that the scaling functions are non-trivial and describe the full non-equilibrium process. The amplitude and the argument J/J_{KZ} scale with powers of the quench rate r_J, with exponents depending only on known static and dynamic critical exponents.

5. Results

We extract the scaling functions $f_A(J/J_{\mathrm{KZ}})$ for $A = M, \chi, \kappa_3, \kappa_4$ by rescaling numerical data with the appropriate amplitudes and powers of r_J; e.g. by rearranging Eq. (10), we obtain $f_M(J/J_{\mathrm{KZ}}) = -\langle M(J, r_J)\rangle / M_0 \bar{r_J}^{\beta/(\beta\delta+\nu z)}$. For the values of the amplitudes and critical exponents, we use the literature values given in [2, 10–12]. Due to the stochastic nature of the equations of motion (2), we take the ensemble averages over $\sim 10k$ statistically independent runs, and extract errors via a bootstrap method. Here, we show results for $d = 2$ dimensions in the infinite volume limit, further results for $d = 3$ and including finite-size scaling can be found in [8].
Fig. 2 shows in the top left panel the evolution $\langle M(J, r_J)\rangle$ of the average order parameter along the trajectory (6) for different quench rates r_J, with the dashed line denoting the equilibrium values. The right side shows the same data with rescaled axes as described before, along with a Padé fit of the scaling function in red. The other rows show the analogous results for χ, κ_3 and κ_4.

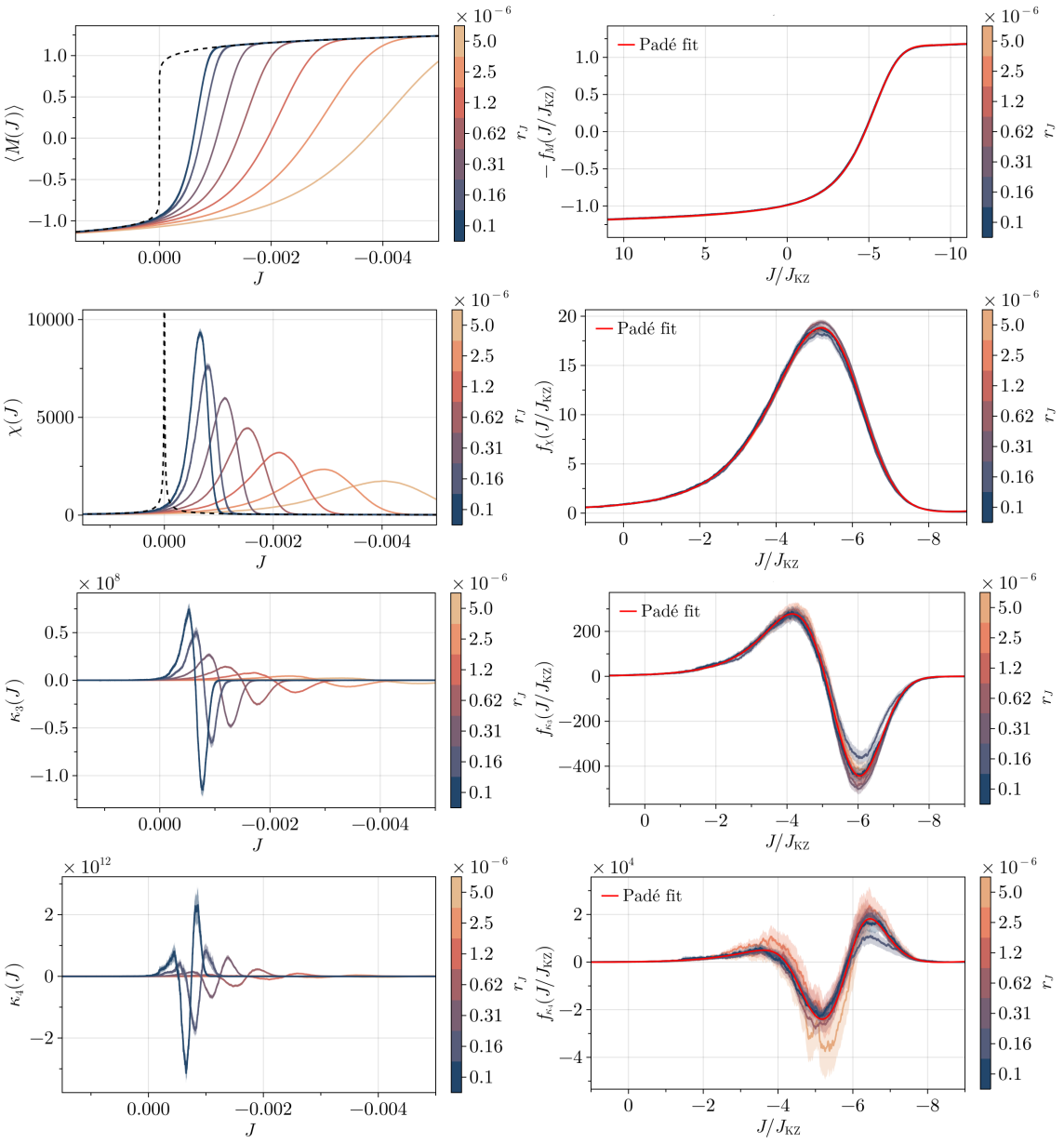

Figure 2: Top left: Average order parameter in $d = 2$ spatial dimensions as function of the external field J in the quench protocol (6) for different quench rates r_J. The dashed line indicates the equilibrium values. Top right: Rescaling of left plot such that the curves collapse onto the universal scaling function $-f_M(J/J_{KZ})$. Padé fit shown in red. Other rows: Analogous results for susceptibility χ and higher cumulants κ_3 and κ_4.

In the left column, one can clearly identify two adiabatic regimes at the start and end of each trajectory, with non-equilibrium evolution in-between. The trajectories differ considerably, depending on how fast the system falls out-of-equilibrum. For high r_J, this happens the fastest, such that the system has less time to react to a change in J, resulting in the more inert response as function of J. The second row left panel in Fig. 2 shows that, at high r_J, the susceptibility maximum decreases, since the system spends less time near the critical point and less fluctuations can build up. Both the size of the non-equilibrium regime and the scale of the cumulants are qualitatively as predicted in

the scaling forms, as e.g. in (10). All curves, irrespective of r_J, show good collapse onto one line representing the universal scaling functions in the right column of Fig. 2. However, the extraction of the higher cumulants is more limited by statistics, such that they exhibit larger error bars.

6. Outlook

We have explicitly demonstrated the emergence of Kibble-Zurek scaling in the non-equilibrium evolution of cumulants of the order parameter in a $\mathbb{Z}_2$ scalar field theory with Model A dynamics and determined the associated scaling functions. In the future, it will be interesting to consider the conjectured dynamic universality class of the QCD critical endpoint, Model H [4], as well as more realistic trajectories in the phase diagram such as, e.g., critical isentropes or quenches across a first-order transition line.

Acknowledgments

We thank Jessica Fuchs, Frederic Klette and Johannes Roth for helpful discussions. This work was supported by the Deutsche Forschungsgemeinschaft (DFG, German Research Foundation) through the CRC-TR 211 'Strong-interaction matter under extreme conditions' – project number 315477589 – TRR 211.

References

[1] M. Bluhm et al., *Dynamics of critical fluctuations: Theory – phenomenology – heavy-ion collisions*, *Nucl. Phys. A* **1003** (2020) 122016 [2001.08831].
[2] A. Pelissetto and E. Vicari, *Critical phenomena and renormalization group theory*, *Phys. Rept.* **368** (2002) 549 [cond-mat/0012164].
[3] P.C. Hohenberg and B.I. Halperin, *Theory of Dynamic Critical Phenomena*, *Rev. Mod. Phys.* **49** (1977) 435.
[4] D.T. Son and M.A. Stephanov, *Dynamic universality class of the QCD critical point*, *Phys. Rev. D* **70** (2004) 056001 [hep-ph/0401052].
[5] T.W.B. Kibble, *Topology of Cosmic Domains and Strings*, *J. Phys. A* **9** (1976) 1387.
[6] W.H. Zurek, *Cosmological Experiments in Superfluid Helium?*, *Nature* **317** (1985) 505.
[7] W.H. Zurek, *Cosmological experiments in condensed matter systems*, *Phys. Rept.* **276** (1996) 177 [cond-mat/9607135].
[8] L.J. Sieke, M. Harhoff, S. Schlichting and L. von Smekal, *Universal non-equilibrium scaling of cumulants across a critical point*, *Nucl. Phys. B* **1011** (2025) 116808 [2411.10266].
[9] D. Schweitzer, S. Schlichting and L. von Smekal, *Spectral functions and dynamic critical behavior of relativistic Z_2 theories*, *Nucl. Phys. B* **960** (2020) 115165 [2007.03374].
[10] F. Kos, D. Poland, D. Simmons-Duffin and A. Vichi, *Precision Islands in the Ising and $O(N)$ Models*, *JHEP* **08** (2016) 036 [1603.04436].
[11] Z. Komargodski and D. Simmons-Duffin, *The Random-Bond Ising Model in 2.01 and 3 Dimensions*, *J. Phys. A* **50** (2017) 154001 [1603.04444].
[12] M.P. Nightingale and H.W.J. Blöte, *Monte carlo computation of correlation times of independent relaxation modes at criticality*, *Phys. Rev. B* **62** (2000) 1089.